Molecular Vision 2020; 26:459-471 <http://www.molvis.org/molvis/v26/459>
Received 19 November 2019 | Accepted 17 June 2020 | Published 19 June 2020

A systems genetics approach to revealing the *Pdgfb* molecular network of the retina

Shasha Li,[1,2] Fuyi Xu,[2] Lin Liu,[1] Rong Ju,[3] Jonas Bergquist,[1,4] Qing Yin Zheng,[5,6] Jia Mi,[1] Lu Lu,[2] Xuri Li,[3] Geng Tian[1]

(The first two authors contributed equally to this work.)

[1]Medicine and Pharmacy Research Center, Binzhou Medical University, Yantai, Shandong, China; [2]Department of Genetics, Genomics and informatics, University of Tennessee Health Science Center, Memphis, TN; [3]State Key Laboratory of Ophthalmology, Zhongshan Ophthalmic Center, Sun Yat-Sen University, Guangzhou, Guangdong, China; [4]Analytical Chemistry and Neurochemistry, Department of Chemistry-BMC, Uppsala University, Uppsala, Sweden; [5]Transformative Otology and Neuroscience Center, Case Western Reserve University School of Medicine, Cleveland, OH; [6]Departments of Otolaryngology, Case Western Reserve University School of Medicine, Cleveland, OH.

Purpose: Platelet-derived growth factor (PDGF) signaling is well known to be involved in vascular retinopathies. Among the PDGF family, the subunit B (PDGFB) protein is considered a promising therapeutic target. This study aimed to identify the genes and potential pathways through which PDGFB affects retinal phenotypes by using a systems genetics approach.

Methods: Gene expression data had been previously generated in a laboratory for the retinas of 75 C57BL/6J(B6) X DBA/2J (BXD) recombinant inbred (RI) strains. Using this data, the genetic correlation method was used to identify genes correlated to *Pdgfb*. A correlation between intraocular pressure (IOP) and *Pdgfb* was calculated based on the Pearson correlation coefficient. A gene set enrichment analysis and the STRING database were used to evaluate gene function and to construct protein–protein interaction (PPI) networks.

Results: *Pdgfb* was a *cis*-regulated gene in the retina; its expression had a significant correlation with IOP (r = 0.305; p value = 0.012). The expression levels of 2,477 genes also had significant correlations with *Pdgfb* expressions ($p<0.05$), among which *Atf4* was the most positively correlated (r = 0.628; p value = 1.29e-10). Thus, *Atf4* was highly expressed in the retina and shared the transcription factor (TF) *Hnf4a* binding site with *Pdgfb*. Gene Ontology and a pathway analysis revealed that *Pdgfb* and its covariates were highly involved in mitogen-activated protein kinase (MAPK) and vascular endothelial growth factor (VEGF) pathways. A generated gene network indicated that *Pdgfb* was directly connected to and interacted with other genes with similar biologic functions.

Conclusions: A systems genetics analysis revealed that *Pdgfb* had significant interactions with *Atf4* and other genes in MAPK and VEGF pathways, through which *Pdgfb* was important in maintaining retina function. These findings provided basic information regarding the *Pdgfb* regulation mechanism and potential therapy for vascular retinopathies.

Platelet-derived growth factor (PDGF) signaling has been implicated in a broad range of vascular retinopathies [1]. Its family consists of four different polypeptide chains encoded by four genes that form five different disulfide-linked dimers: PDGF-AA, PDGF-AB, PDGF-BB, PDGF-CC, and PDGF-DD. They act using two receptor tyrosine kinases: the PDGF receptors (PDGFRs) alpha and beta. Due to their functions in retinopathies, targeted PDGF family members have exhibited potential therapeutic values regarding the diseases [2]. Among these isoforms, *PDGFB* (Gene ID: 5155, OMIM: 190040) is considered a key regulator of retina diseases and a potential therapeutic target [3,4]. It is a paracrine signal from endothelial cells to pericytes, which are important in regards to capillary morphogenesis in the retina [5]. Indeed, the PDGF-AB complex concentration has been shown to be significantly elevated in patients with diabetes and age-related macular degeneration (AMD) [6]. Further, signaling induced by *Pdgfb* has been reported to be related to PDGFB/PDGFRβ signaling, which is critical to the formation and maturation of the blood–retinal barrier through the active recruitment of pericytes onto growing retinal vessels [7]. Studies of mice have shown that *Pdgfb* can be a neuroprotector against light-induced photoreceptor damage [8] and that the overexpression of *Pdgfb* in mice has phenotypes similar to diabetic retinopathy [2]. Recent evidence has suggested the ability to simultaneously inhibit VEGF and PDGF to ameliorate AMD; however, clinical trials have not been successful [9]. This could be due to the propensity of PDGF and VEGF family members to form complex regulatory networks [10].

Correspondence to: Geng Tian, Medicine and Pharmacy Research Center, Binzhou Medical University, Yantai, Shandong, China; Phone: +86-535-6913395; FAX: +86-535-6913034; email: tiangeng@live.se

Thus, it is critical to investigate *Pdgfb* correlated genes and the related co-expression network to understand the function of *Pdgfb* in the retina.

A systems genetics approach is a unique method for investigating a gene's coexpression networks. With well-maintained recombinant inbred (RI) strains of mice, a combinatorial application of genomics, transcriptomics, proteomics, and metabolomics can provide detailed insights into gene transcription regulation and subsequent coexpression networks for a gene of interest. Currently, one of the largest panels of RI mouse strains is the BXD family, which consists of more than 150 strains derived from a cross between the C57BL/6J (B6) and DBA/2J (D2) strains. While each line is fully inbred, the entire collection is highly diverse. Many studies of genetic networks have used the BXD RI strains of mice [11-14]. Moreover, the BXD lines have been used extensively in studies that have aimed to identify the genetic bases of ocular phenotypes [15]. Therefore, these strains have a unique foundation with which *Pdgfb* has been investigated using a systems genetics approach.

This study aimed to assess the expressions and resulting regulatory networks of genes belonging to the PDGF and VEGF families in the retina; it aimed to do so with a systems genetics approach. The intent was to identify the expression quantitative trait locus (eQTL) of *Pdgfb,* analyze its potential pathways, and construct a genetic network that could contribute to retinal diseases. The data offered several novel putative *Pdgfb* correlated genes and a novel PDGFB regulatory network in the retina.

METHODS

Generating retinal gene expression data from BXD mice: The gene expression data generated in this study can be accessed through the "Full HEI Retina Illumina V6.2 (Apr10) RankInv" dataset at the website GeneNetwork [11]. The sections below briefly describe the data generation process.

Animals: BXD mice and their parental strains B6 and D2 were bred at the University of Tennessee Health Science Center (Memphis, Tennessee). The animals were fed chow ad libitum and maintained on a 12 h:12 h light-dark cycle. The animal experiment protocols were approved by the Institutional Animal Care and Use Committee of the University of Tennessee Health Science Center. The mice were handled in conformance with the ARVO Statement for the Use of Animals in Ophthalmic and Vision Research and the Guide for the Care and Use of Laboratory Animals from the Institute of Laboratory Animal Resources (the Public Health Service policy on the humane care and use of laboratory animals).

Tissue harvesting and RNA extractions: Animals 60 to 90 days old were sacrificed using rapid cervical dislocation. After being anesthetized with an IP injection of ketamine, xylazine, and acepromazine at doses of 40, 5, and 1 mg/kg, respectively. From each mouse, two retinas were immediately isolated; they were placed in RNAlater (Applied Biosystems, Foster City, CA), and stored in a single tube overnight at 4 °C, followed by a minimum of 24 h of freezing at −20 °C and long-term storage at −80 °C. Total RNA was extracted from the retinas using the RNA STAT-60 method (Tel-Test Inc., Amsbio, Abingdon, UK) following the manufacturer's instructions. Briefly, the tissues were homogenized in RNA STAT-60 (1 ml per 50 mg to 100 mg of tissue) with a syringe, followed by an addition of 0.2 ml of chloroform and centrifugation at 12,000 ×*g* for 1 h at 4 °C. The aqueous phase was transferred into a clean centrifuge tube and incubated with 0.5 ml of isopropanol for 1 h or overnight at −20 °C. After centrifugation at 12,000 ×*g* for 1 h, the RNA was washed with 75% ethanol and dissolved in 50 µl of nuclease free water (Qiagen, Hilden, Germany). The quality and purity of the RNA was assessed using the Agilent 2100 Bioanalyzer system (Agilent, Santa Clara, CA). RNA samples with an RNA integrity number of eight or higher were selected for further analyses.

Microarrays and data processing: The gene expression data used in this study were obtained using Illumina MouseWG-6 v2.0 arrays (Illumina, San Diego, CA) following the manufacturer's protocol. Briefly, Total RNA was processed with the Illumina TotalPrep RNA Amplification Kit (Applied Biosystems, Foster City, CA) to produce biotinylated complementary-RNAs (cRNAs). This procedure included the reverse transcription of RNA to synthesize the first strand complementary-DNA (cDNA), second strand cDNA synthesis, cDNA purification, in vitro transcription to synthesize cRNA, cRNA amplification, and purification. The biotinylated cRNAs were hybridized to the Illumina Sentrix® Mouse Whole Genome-6 version 2.0 arrays (Illumina) for 19.5 h at 58 °C. The detailed info for RNA extraction and Array hybridization can be found in our previous publication [16]. This dataset included data from 75 BXD strains, their parental strains B6 and D2, and both reciprocal F1 hybrids between B6 and D2, with an average of four samples for each strain (including a roughly equal number of males and females). Raw microarray data were normalized using a rank-invariant method and background subtraction protocols provided by Illumina as a part of the BeadStation software suite (Illumina). In short, the individual p-values was sorted in ascending order, then a rank was assigned for each p-values. The B-H critical value was calculated using the formula formula (i/m) Q, where:

- i = the individual p-value's rank,
- m = total number of tests,
- Q = the false discovery rate (0.05)

The original p-value was compare to the critical B-H value, and find the largest p value that is smaller than the critical value. The expression data were then renormalized using a modified Z score described in a previous publication [17]. Briefly, log base two was calculated for the normalized values, the Z scores for each array were calculated, the Z scores were multiplied by two, and an offset of eight units was added to each value. This transformation yielded a set of Z-like scores for each array with a mean of eight, a variance of four, and a standard deviation of two.

Intraocular pressure (IOP) measurements: The IOP of each mouse was measured at the age of six to eight weeks, with an average of eight mice for each strain. The mice were mildly anesthetized with isoflurane (Alfa Aesa, Haverhill, MA), then the IOP was measured from 10:00 a.m. to 4:00 p.m. during the light cycle using an induced impact tonometer (Tonolab, Colonial Medical Supply, Franconia, New Hampshire). The IOP values for the left and right eyes were then averaged. The dataset can be retrieved from a database server with the record ID 12,300 (GeneNetwork).

eQTL mapping: eQTL mapping was conducted using a WebQTL module in GeneNetwork software (GeneNetwork) using published methods [17]. Briefly, the methodology used regression analyses to determine relationships between differences in a trait and relationships between differences in alleles at markers across a genome. Simple interval mapping was performed to identify potential eQTLs that regulated *Pdgfb* expression levels and to estimate significance at each location using known genotype data for sites. In addition, composite interval mapping was used to map secondary genetic loci by controlling genetic variances associated with a major eQTL. Both analyses produced likelihood ratio statistics (LRSs); quantitative measurements of links between observed phenotypes, which were variations in expression levels of *Pdgfb*; and known genetic markers. A genome-wide significance ($p<0.05$) for each eQTL was established using a permutation test that compared the LRS values of the novel site with the LRS values of 1,000 genetic permutations; other parameters were left as defaults.

Sequence variant analyses: The genetic variants of *Pdgfb*, including single nucleotide polymorphisms (SNPs) and small insertions and deletions (indels) between the parental strains B6 and D2, were determined using the Mouse Genomes Project (Mouse_SnpViewer) variant querying site [18]. Briefly, we searched the genetic variants for *Pdgfb* at Sanger Mouse SNP Viewer with default settings, except for the "strains" option, where only DBA2/J (D2) was selected (mouse-genomes-project).

Gene set enrichment analyses: The Pearson correlation coefficients of strain means between expressions of *Pdgfb* and all other probe sets were computed across the mouse genome to produce sets of genetically correlated genes. Next, a literature correlation analysis was performed to rank the list of genes using the software Semantic Gene Organizer, which automatically extracted gene correlations from the titles and abstracts of MEDLINE citations [19]. All genetic and literature correlations were computed using GeneNetwork. Briefly, genes with significant genetic correlations ($p<0.05$) and literature correlations ($r>0.3$) with *Pdgfb*, as well as mean expression levels of >7.0, were selected and uploaded to the open source analysis tools on Webgestalt [20]. This was done for Gene Ontology (GO; biologic processes) Kyoto Encyclopedia of Genes and Genomes (KEGG) pathway analyses and transcription factor (TF) target over-representation analyses. The mouse genome was used as the reference gene set. The p values generated from hypergeometric tests were automatically adjusted to account for multiple comparisons using the Benjamini and Hochberg correction method [21] . This calculation was automatically obtained from Webgestalt [20] with the formula (i/m) Q, where i is the individual p-value's rank, m is the total number of tests, and Q is the false discovery rate. Categories with adjusted p values of <0.05 indicated that the set of submitted genes was significantly over-represented in those categories.

Protein–protein interaction (PPI) network constructions: PPI networks provided valuable information for understanding cellular functions and biologic processes. The gene set was submitted to the online tool STRING [22], a database of known and predicted PPIs. The direct PDGFB PPI network was then retrieved with an interaction score of >0.4 (a median confidence).

RESULTS

Significant correlation of Pdgfb with IOP: To identify the associations of related traits with growth factors from the PDGF family, a correlation screening was performed using the currently known members of the PDGF and VEGF families in regards to the IOP. Among the various members of the families, *Pdgfb* was the only member that was significantly correlated with IOP ($r = 0.305$; $p = 0.012$; Figure 1A). The IOP ranged between 11.643 and 19.833 mmHg, with a median of 15.500 mmHg (Figure 1B).

Pdgfb expression levels in the retinas of BXD mice: The *Pdgfb* expression profile was further investigated across the

BXD strains. The *Pdgfb* expressions varied significantly across the BXD strains with a fold change of 1.73 (Figure 2). The average expression of *Pdgfb* across all the BXD strains was 7.66 ± 0.02 (log2 scale, mean ± SEM), such that BXD16 showed the highest expression (8.09 ± 0.14) and BXD71 showed the lowest expression (7.29 ± 0.12). This indicated that the genetic variability influenced the *Pdgfb* expressions and thereby facilitated the identification of loci that controlled the *Pdgfb* expressions among the BXD mice strains.

eQTL mapping and the sequence variants of Pdgfb: To identify the genetic loci that regulated *Pdgfb* expressions in the retina tissues, simple interval mapping was performed for *Pdgfb* across the mouse genome. The results showed a significant eQTL on chromosome 15 at 80.25 Mb with an LRS of 39.3, which was close to the physical location of *Pdgfb* on chromosome 15 at 80.00 Mb (Figure 3). Further composite interval mapping revealed no secondary genetic loci that modulated *Pdgfb* expressions. This indicated that *Pdgfb* was a *cis*-regulated gene, which suggested that a variation in *Pdgfb* expression was caused by genetic variants nearby or within the *Pdgfb* gene. Further, a search for mouse genome variants from the Mouse Genomes Project yielded a total of 165 genetic variants in *Pdgfb* between the BXD parental strains, including SNPs and indels. Among them, 18 variants were defined as 5′-UTR UTR-3′ synonymous or splice variants (Table 1), while the rest were all intron variants. The 5'- untranslated region (UTR) and 3'-UTR we mentioned in the text are genomic regions rather than primers. 5' UTR is the portion of an mRNA from the 5' end to the position of the first codon used in translation. The 3' UTR is the portion of an mRNA from the 3' end of the mRNA to the position of the last codon used in translation. Some of these variants could have been responsible for the variable *Pdgfb* expression in the BXD mice.

Pdgfb correlated genes and gene function enrichment analyses: After filtering was conducted based on a mean expression value, genetic correlation, and literature correlation, a total of 2,477 genes ($p<0.05$) were identified as correlated with *Pdgfb* (Appendix 1). The top ten positively and negatively correlated genes are listed in Table 2. Among them, *Atf4* was expressed significantly in the retinas, and it was the top gene positively correlated with *Pdgfb* (r = 0.628; p = 1.29e-10; Figure 4). To explore the functional relationship between *Atf4* and *Pdgfb*, a TF target enrichment analysis was performed and three motifs were identified: CTGCAGY, RAAGNYNNCTTY, and TGAMCTTTGMMCYT. They

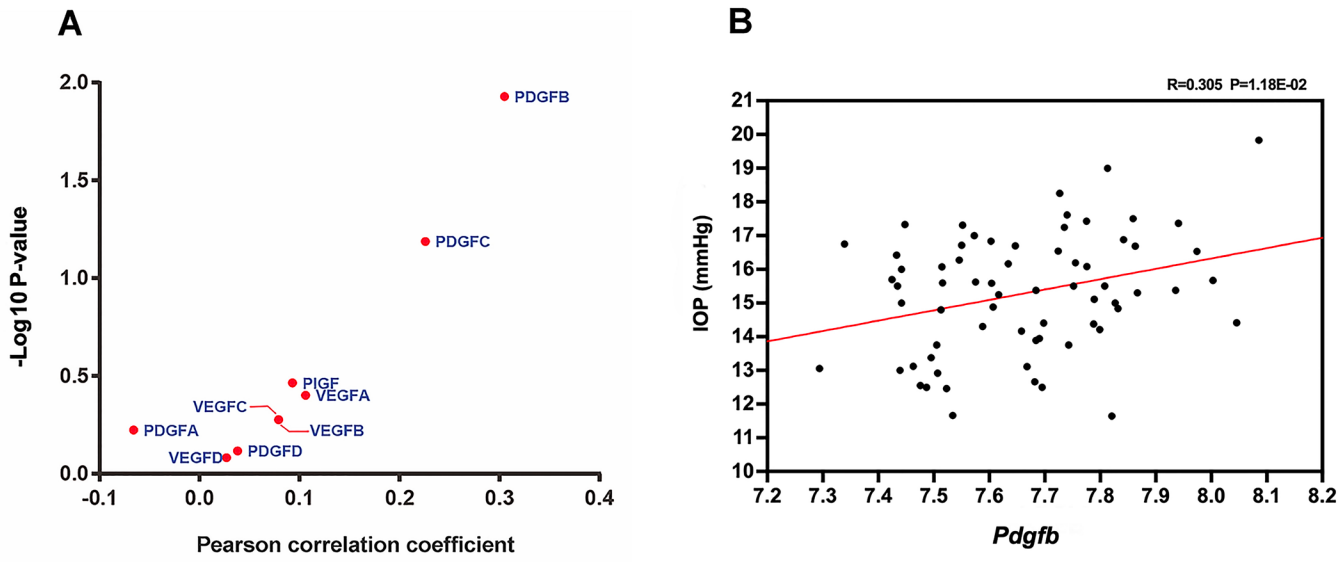

Figure 1. Expression of *Pdgfb* correlated with intraocular pressure (IOP). **A**: A volcano plot was created for Pearson correlations between IOP and members of the platelet-derived growth factor (PDGF) and vascular endothelial growth factor (VEGF) families across the BXD strains. The y-axis represented the log10 transformed p value of each correlation coefficient. The x-axis represented the correlation coefficient. Each spot represented a member of the PDGF family or the VEGF family. Among the various members of the families, *Pdgfb* was the only member significantly correlated with IOP. **B**: A scatterplot was created for correlations of IOP (y-axis) with expression levels of *Pdgfb* (x-axis) among the BXD strains. Each spot represented a BXD strain or its parental strain. There was a statistically significant positive correlation between the expression of *Pdgfb* and IOP (r = 0.305; p = 0.012). IOP was measured for mice of both sexes about two months old, and the value that was represented was the average for the left and right eyes.

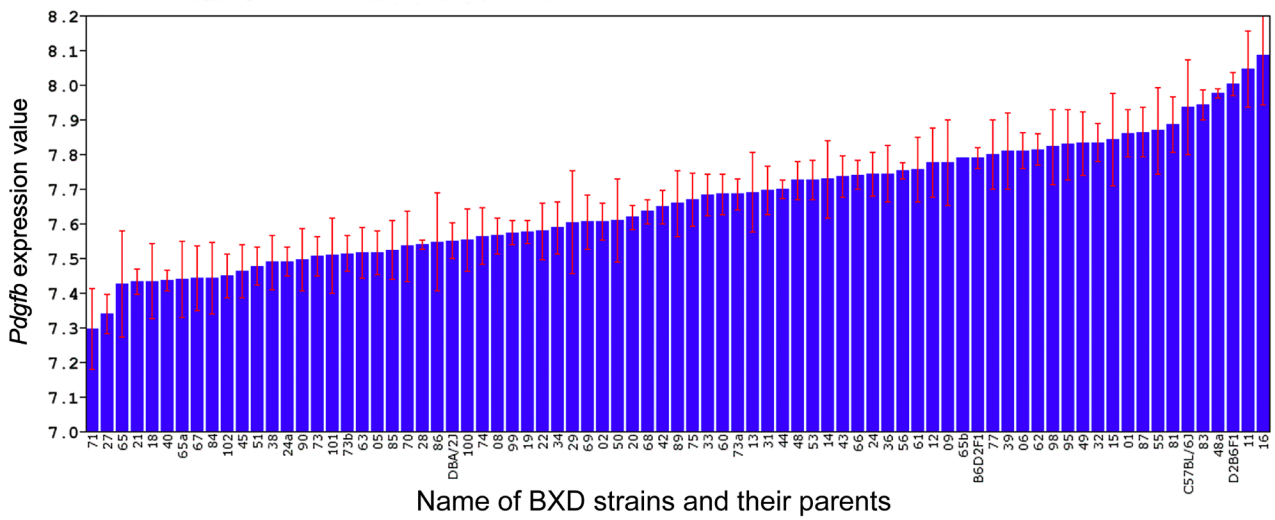

Figure 2. The expression level of Pdgfb in the retina tissue for 75 BXD strains, two F1 strains (B6D2F1 and D2B6F1), and parental strains (B6 and D2) were represented. The expression level ranges from 7.29 ± 0.12, BXD71 to 8.09 ± 0.14, BXD 16. The mean expression of *Pdgfb* across all the BXD strains was 7.66 ± 0.02, with BXD16 showed the highest expression and BXD71 showed the lowest expression. The x-axis denoted strain's name, while the y-axis denoted the mean expression given in a log2. Each bar showed mean expression values ± the standard error of the mean (SEM).

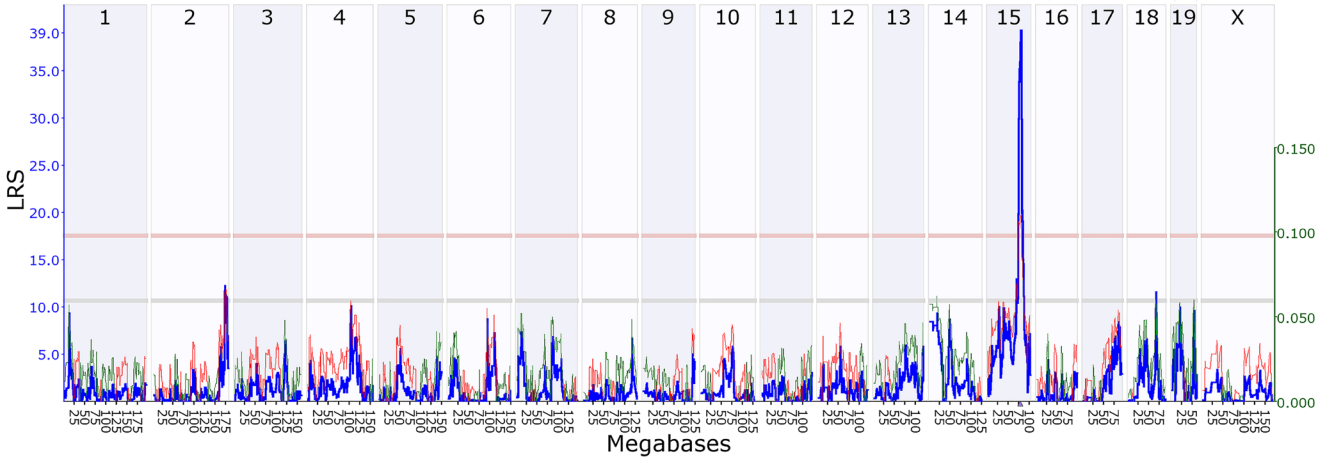

Figure 3. The interval mapping of *Pdgfb* in the retina was represented. A genome-wide significant expression quantitative trait locus (eQTL) was present on chromosome 15 at 80.25 Mb, which was close to the physical position of *Pdgfb* on chromosome 15 at 80.00 Mb and made it a *cis*-eQTL. The upper x-axis showed the chromosome, and the lower x-axis showed the location in megabases. The left y-axis provided a likelihood ratio statistics (LRS) score in blue, and the right y-axis provided an additive effect. The red and green lines showed the effects of the D and B alleles on trait values, respectively. The two horizontal lines across the plot made the genome-wide thresholds significant ($p<0.05$, the pink or upper line) and suggestive ($p<0.63$, the gray or lower line).

were colocated in the transcription start sites of *Atf4* and *Pdgfb* (FDR p<0.05). However, according to the TRANSFAC database, the first two motifs did not match any known TF binding sites, but the last motif did match the annotation for HNF4A. That is, the gene encoded hepatic nuclear factor 4 alpha, which was essential for maintaining normal vision and eye phenotypes. According to Mouse Genome Informatics and the International Mouse Phenotyping Consortium (IMPC), mice that carry a null allele of this gene have abnormal retinal vasculatures, retinal blood vessels, and lens morphologies and increased total retina thicknesses and cataracts.

To further evaluate the gene function of the *Pdgfb* correlated genes, 2,477 genes were submitted to Webgestalt to perform GO and KEGG pathway enrichment analyses. The gene set was found to be significantly associated with the development of blood vessels, eyes, and retinas (Table 3). Furthermore, according to the KEGG pathway enrichment analyses, several pathways involved in AMD were overrepresented, including the MAPK signaling pathway, the PI3K-Akt signaling pathway and the apoptosis pathway (Table 3).

PPI network analyses: To further identify the proteins that directly interacted with PDGFB and its network, the gene set of 2,477 genes was submitted to the STRING database. The results showed that 45 proteins directly interacted with PDGFB, among which 17 proteins were already implicated in eye and vision related traits, according to mammalian phenotype ontology. These included CTGF, EGF, EGFR, FGFR1, FGFR2, HIF1A, JAG1, KDR, KIT, NRP1, PDGFC, PR1R, PTEN, S1C20A2, TGFB1, TRP53, and VEGFB (Figure 5).

DISCUSSION

Correlations between members of the PDGF and VEGF families and IOP, a major risk factor for vascular retinopathy, were evaluated. Among the members of these families, *Pdgfb* was the only gene in the retina with an expression that correlated with IOP. Previous reports indicated elevated levels of *Pdgfb* in the plasma of neovascular AMD individuals [23]. Moreover, several genetic markers for IOP were suggested in population GWAS studies [24]. However, the genetic markers of *Pdgfb* had not yet been elucidated. In the present study of BXD mouse strains, a significant correlation was identified between the expression of *Pdgfb* and IOP. This result agreed with the neuroprotection function of *Pdgfb* in physiologic conditions [25]; it had been found that in animal models, a high retinal expression of *Pdgfb* resulted in a tractional retinal detachment due to a proliferation of vascular and nonvascular cells, similar to diabetic retinopathy in humans [2]. Thus, the present study's results indicated the importance of *Pdgfb* in regards to retinal vascular disease and thereby reinforced the possibility of targeting *Pdgfb* for the treatment of AMD and glaucoma.

Table 1. The genetic variants (SNPs and indels) of the PDGFB gene.

Chr	Position	dbSNP	Ref	DBA/2J	Variant Type
15	79,996,113	rs13473669	T	G	3_prime_utr_variant
15	79,996,211	rs13473671	A	C	3_prime_utr_variant
15	79,996,551	rs31860371	G	A	3_prime_utr_variant
15	79,996,691	rs37125180	C	T	3_prime_utr_variant
15	79,996,737	-	T	C	3_prime_utr_variant
15	79,996,738	rs31659446	G	T	3_prime_utr_variant
15	79,996,960	rs38861363	G	A	3_prime_utr_variant
15	79,997,082	rs3023421	C	G	3_prime_utr_variant
15	79,997,106	rs3090582	A	G	3_prime_utr_variant
15	80,001,817	rs37855405	A	C	synonymous_variant
15	80,013,951	rs46685607	A	G	synonymous_variant
15	80,014,069	rs31754859	T	G	5_prime_utr_variant
15	80,014,120	rs52143023	A	C	5_prime_utr_variant
15	80,014,377	rs31674526	G	T	5_prime_utr_variant
15	80,014,465	rs31919564	G	A	5_prime_utr_variant
15	79,995,959	rs220772058	C	CA	3_prime_utr_variant
15	79,996,992	rs245144653	AGTCCAC	A	3_prime_utr_variant
15	79,997,711	rs235158122	GAGA	G	splice_region_variant

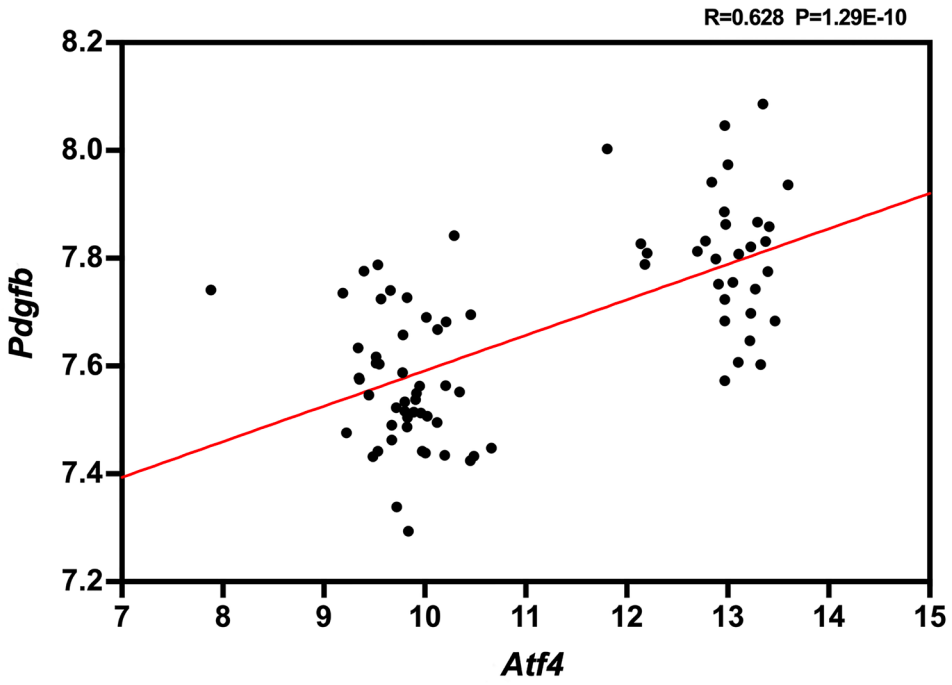

Figure 4. A scatterplot was created for *Pdgfb* and expression correlations with *Atf4* among the BXD strains. Each spot represented one BXD strain or its parental strain. The expression of *Pdgfb* genes had a statistically significant positive correlation with the expression of *Atf4* genes (r = 0.628, p = 1.29e-10).

Table 2. Top 10 genes positively and negatively correlated with PDGFB.

Symbol	Gene ID	Chr	Mb	Mean Expression	r	P value
Atf4	11,911	15	80.25626	11.032	0.636	2.57E-10
Mgat3	17,309	15	80.21522	8.622	0.629	4.59E-10
Ltbp4	108,075	7	27.30542	8.095	0.584	1.79E-08
Smtn	29,856	11	3.517692	8.997	0.56	9.76E-08
Rassf2	215,653	2	131.9932	7.374	0.543	2.86E-07
Marveld1	277,010	19	42.15104	7.483	0.543	2.97E-07
Klf2	16,598	8	72.32098	7.688	0.536	4.71E-07
Xrcc6	14,375	15	82.03751	9.575	0.528	7.36E-07
Nol12	97,961	15	78.93783	9.465	0.524	9.4E-07
Itga7	16,404	10	128.9578	7.222	0.523	0.000001
Clcn3	12,725	8	60.95465	7.31	−0.642	1.46E-10
1810044A24Rik	76,510	15	72.79971	7.422	−0.5	3.77E-06
Hdgf	15,191	3	87.91495	8.121	−0.494	5.09E-06
Ranbp2	19,386	10	58.46073	7.73	−0.49	6.42E-06
Arid4a	238,247	12	71.07602	7.663	−0.489	6.75E-06
Phf14	75,725	6	11.93326	10.163	−0.486	7.57E-06
Eno1	13,806	4	150.2466	12.026	−0.481	1.01E-05
Klf9	16,601	19	23.16632	14.303	−0.48	1.08E-05
Araf	11,836	X	20.8526	10.008	−0.479	1.1E-05
Cbx3	12,417	1	58.64664	7.04	−0.471	1.66E-05

Table 3. Significant enriched terms for GO and KEGG pathways.

Gene Set	Description	N. of Gene	P Value	FDR
GO (biologic process)				
GO:0001568	blood vessel development	146	0	0
GO:0001654	eye development	92	1.78E-15	6.04E-14
GO:0043010	camera-type eye development	80	1.06E-13	3.01E-12
GO:0060041	retina development in camera-type eye	45	1.05E-10	2.13E-09
GO:0048592	eye morphogenesis	40	1.48E-07	1.71E-06
GO:0048593	camera-type eye morphogenesis	28	3.19E-05	0.000233
GO:0003407	neural retina development	17	8.78E-05	0.000565
GO:0001754	eye photoreceptor cell differentiation	15	0.000126	0.000774
GO:0042462	eye photoreceptor cell development	12	0.000301	0.001645
GO:0031290	retinal ganglion cell axon guidance	8	0.000521	0.002611
GO:0002088	lens development in camera-type eye	17	0.001044	0.004746
GO:0031076	embryonic camera-type eye development	11	0.003103	0.0118
GO:0060042	retina morphogenesis in camera-type eye	13	0.004078	0.01461
GO:0048596	embryonic camera-type eye morphogenesis	8	0.008698	0.02801
GO:0061298	retina vasculature development in camera-type eye	6	0.001344	0.03964
KEGG pathway				
mmu04010	MAPK signaling pathway	86	4.84E-14	4.82E-12
mmu04151	PI3K-Akt signaling pathway	90	9.99E-08	4.98E-06
mmu04210	Apoptosis	43	1.96E-06	3.91E-05
mmu04014	Ras signaling pathway	62	3.22E-06	5.67E-05
mmu04066	HIF-1 signaling pathway	34	2.23E-05	0.000256
mmu04350	TGF-beta signaling pathway	28	3.89E-05	0.000401
mmu04150	mTOR signaling pathway	42	0.000126	0.001018
mmu04024	cAMP signaling pathway	48	0.000714	0.00368
mmu04370	VEGF signaling pathway	18	0.002992	0.01278
mmu04310	Wnt signaling pathway	35	0.003964	0.01559

In addition to the known *Pdgfb* correlated regulators, the results of the gene correlation analysis suggested a group of putative *Pdgfb* correlated genes. Among them, *Atf4* was expressed significantly in the retinas and was the top gene positively correlated with *Pdgfb*. In addition, expressions of *Atf4* and *Pdgfb* had significant correlations in many human tissues (Appendix 2). *Atf4* was characterized as cAMP-response element binding protein 2 (CRBP2), a DNA binding protein widely expressed in mammals [26]. The function of *Atf4* in normal and malignant cells was related to stress-induced transcription activation [27]. In smooth muscle cells, *Pdgfb* could mediate cell migration through *Atf4* [28]. However, the relationship between *Atf4* and *Pdgfb* in the retina remained unclear.

One potential mechanism was that *Atf4* and *Pdgfb* shared common transcriptional factor binding motifs and were thus coexpressed. In the TF binding enrichment analysis, *Hnf4a* was identified as a shared TF for both *Atf4* and *Pdgfb*. Mice with null *Hnf4a* presented retina disorders, but the mechanism remained unclear. The results indicated a potential mechanism through the PDGFB pathway.

Another shared regulator could be noncoding RNAs. MicroRNA-214 (miR-214) was a microRNA that regulated ocular neovascularization [29]. Both *Atf4* and *Pdgfb* were known targets of miR-214. Moreover, miR-214 inhibited vascularization through a reduced *Pdgfb* release, and a suppression of miR-214 could increase an *Atf4* level [30]. However, the detailed mechanisms needed to be further illustrated. Augmented *Atf4* signals that occurred during retinal degeneration had cytotoxic roles by triggering photoreceptor cell death [31]. *Atf4* was overexpressed in retinas that suffered from oxygen-induced retinopathy, and its inhibition

had been reported to prevent pathologic neovascularization [32]. Furthermore, *Atf4* had been reported to bind to a VEGF promoter [33], which suggested a complicated regulatory network involving ATF4-PDGFB-VEGF. The results indicated a critical function of *Atf4* in regards to *Pdgfb* and VEGF in the retina.

One of the top genes negatively correlated with *Pdgfb* was *Hdgf*. Although the cross-regulation of *Pdgfb* and *Hdgf* remained unclear, *Hdgf* had been found to display a functional similarity with *Pdgfb*. *Hdgf* had stimulated smooth muscle cell growth and had acted as a mitogen for various types of cells. It had also recently been identified as an angiogenic factor that regulated the retinal vasculature in physiological and pathological conditions [34]. In injured retinal ganglion cells, HDGF could have a neuroprotective role [35]. Thus, the negative correlation between *Hdgf* and *Pdgfb* indicated

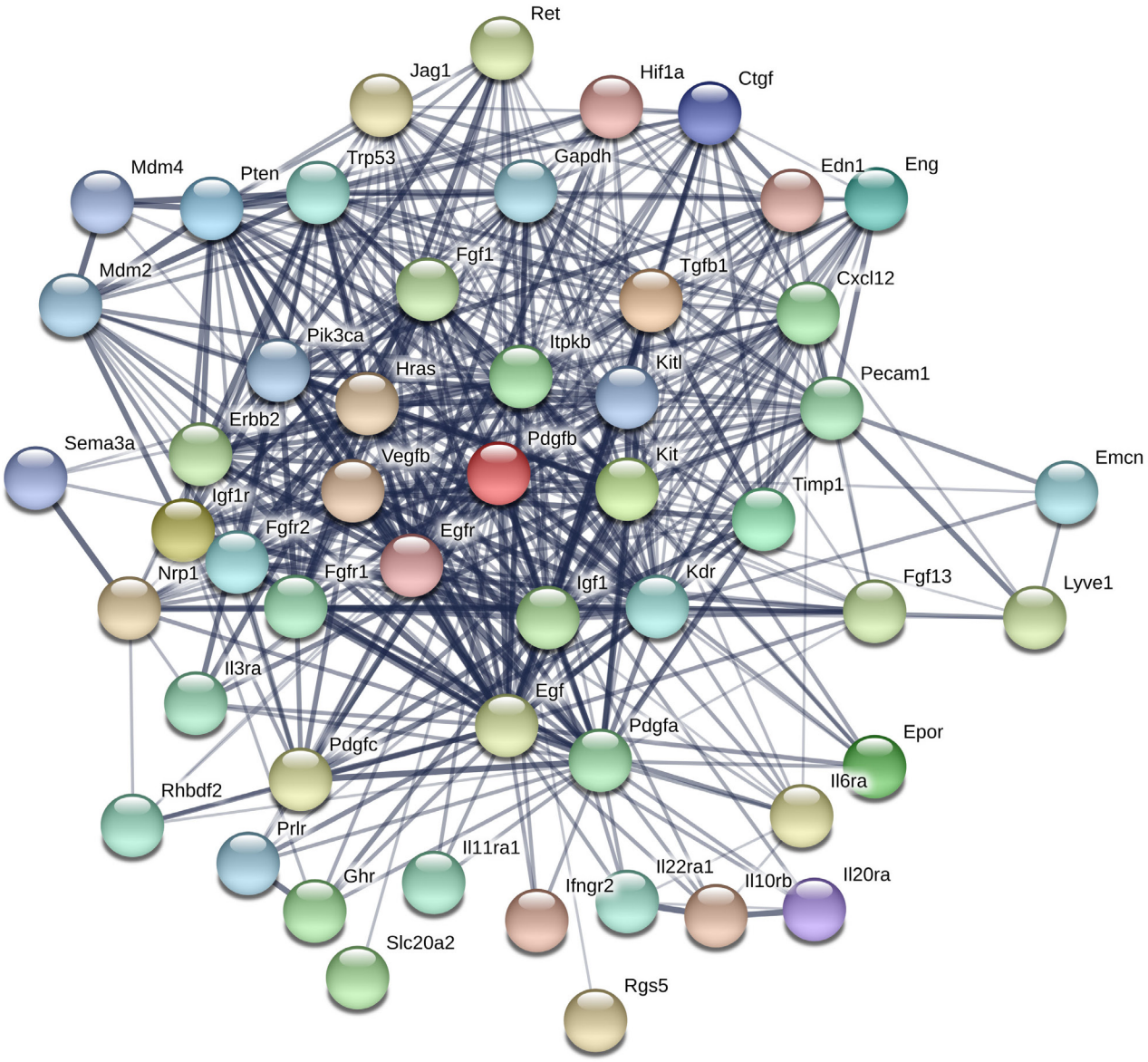

Figure 5. The protein-protein interaction (PPI) network of *Pdgfb* was represented. A *Pdgfb* involved PPI network was retrieved from the online tool STRING with an interaction score of > 0.4 (a median confidence). According to mammalian phenotype ontology, 45 proteins were reported as directly interacted with Pdgfb, among which 17 proteins were already implicated in eye and visual-related traits. Nodes represented proteins and edges represented the interaction confidence between two nodes.

potential compensatory roles for the two growth factors. However, more studies were needed to elucidate the detailed mechanism.

A gene enrichment analysis was used to identify the GO categories in which *Pdgfb* and its correlated genes were over-represented and to identify the pathways through which they had roles in regards to the retina. The GO analysis showed that *Pdgfb* correlated genes were significantly involved in blood vessel development, retina development, differentiation, and morphogenesis. This confirmed the major functions of *Pdgfb* and its correlated genes in the retina. Further, the gene pathway enrichment analysis indicated MAPK as the topmost signaling pathway, and this result agreed with a previous study that showed *Pdgfb* had the ability to activate the MAPK pathway [36]. Moreover, in the present study, it was found that 98 other *Pdgfb* correlated genes were located in the MAPK pathway, and *Pdgfb* interacted with them to maintain various functions, such as angiogenesis and cell survival.

Finally, the VEGF signaling pathway was one of the top enriched pathways. The cross interaction between VEGF and PDGF signaling had been noted in previous studies [37], and PDGF signaling had been suggested to be partially responsible for resistance to VEGF targeting therapy. Thus, the present study's results confirmed this cross-family interaction in the retina and therefore provided a helpful resource for further investigations into VEGF-PDGF signaling interactions.

To further illustrate the function of the *Pdgfb* correlated genes at the protein level, a PPI network analysis was performed. The PPI analysis provided protein interaction information for the gene products. As a result, 57 gene products were reported to have directly interacted with PDGFB, among which 17 proteins were involved in eye diseases. Intriguingly, most of these proteins were growth factors and corresponding receptors. These results indicated a complex growth factor cotranscription regulatory network. In particular, two members from the PDGF family, PDGFA and PDGFC, had significant correlations with PDGFB, which confirmed that the PDGF family was involved in the regulation of PDGFB expressions. Further, a correlation with the VEGF family member VEGFB was found. Growth factors from the VEGF and PDGF families were promising therapeutic targets for major vascular retinopathies. The co-expression network could provide novel leads for therapy and drug design, and this work confirmed that the complicated gene network of the VEGF-PDGF interaction had a critical role in the retina.

Conclusions: With a systematic analysis that involved more than 70 mouse strains, it was found that a *Pdgfb* expression in the retina was highly variable and correlated significantly with IOP. A *Pdgfb* coexpression network revealed a complicated network of growth factors in the retina, and *Atf4* and *Hdgf* were potential novel genes that interacted with *Pdgfb* in the retina. Further gene ontology and pathway analyses indicated that many of these genes interacted with the MAPK and VEGF pathways and thus provided the putative *Pdgfb* action mechanism of mediating cell survival and providing neuroprotection. Thus, the study confirmed the importance of *Pdgfb* in retinopathies. However, it was noted that further investigations should be conducted to elucidate the nature and underlying mechanisms of these relationships and assist in the development of efficacious treatment strategies for retinal vascular diseases.

APPENDIX 1: THE LIST OF 2477 GENES (P<0.05) CORRELATED WITH *PDGFB*.

To access the data, click or select the words "Appendix 1."

APPENDIX 2. SCATTERPLOT OF CORRELATION BETWEEN THE EXPRESSION OF *ATF4* AND *PDGFB* IN THE HUMAN TISSUES FROM HUMAN GTEX DATA SET.

To access the data, click or select the words "Appendix 2." y-axis indicates Log2 transformed value of transcripts per million (TPM) for *PDGFB*. x-axis indicates Log2 transformed TPM for *ATF4*. Each dot represents an individual sample. The analysis included 8587 samples from 53 tissues from GTEx project. The full list of tissue name is provided in Appendix 3. The Pearson correlation analysis was performed with online GTEx analysis tool Gepia. The result showed that the expression of *ATF4* and *PDGFB* is significantly correlated at a pan-tissue level (r=0.32, p=0, n=8587).

APPENDIX 3: THE FULL LIST OF GTEX TISSUE NAME.

To access the data, click or select the words "Appendix 3."

ACKNOWLEDGMENTS

The research was supported by Taishan Scholars Construction Engineering (G.T.), National Natural Science Foundation of China (31771284, 81670855), Open Research Funds of the State Key Laboratory of Ophthalmology (G.T. and X.L.), Science and Technology Support Plan for Youth Innovation of Higher Education of Shandong (2019KJE013), the Key Research and Development Plan of Shandong Province (2016GSF201100, 2018GSF118230), Shandong Provincial Natural Science Foundation(ZR2016JL026), Swedish Research Council

grant 2015-4870 (JB), A grant from National Institutes of Health of United States (R01DC015111). The authors would like to express their gratitude to EditSprings (https://www.editsprings.com/) for the expert linguistic services provided. Dr. Geng Tian (tiangeng@live.se) and Dr. Xuri Li (lixr6@mail.sysu.edu.cn) are co-corresponding authors for this paper.

REFERENCES

1. Andrae J, Gallini R, Betsholtz C. Role of platelet-derived growth factors in physiology and medicine. Genes Dev 2008; 22:1276-312. [PMID: 18483217].
2. Mori K, Gehlbach P, Ando A, Dyer G, Lipinsky E, Chaudhry AG, Hackett SF, Campochiaro PA. Retina-specific expression of PDGF-B versus PDGF-A: vascular versus nonvascular proliferative retinopathy. Invest Ophthalmol Vis Sci 2002; 43:2001-6. [PMID: 12037011].
3. Lindahl P, Johansson BR, Leveen P, Betsholtz C. Pericyte loss and microaneurysm formation in PDGF-B-deficient mice. Science 1997; 277:242-5. [PMID: 9211853].
4. Jaffe GJ, Ciulla TA, Ciardella AP, Devin F, Dugel PU, Eandi CM, Masonson H, Monés J, Pearlman JA, Quaranta-El Maftouhi M, Ricci F, Westby K, Patel SC. Dual Antagonism of PDGF and VEGF in Neovascular Age-Related Macular Degeneration: A Phase IIb, Multicenter, Randomized Controlled Trial. Ophthalmology 2017; 124:224-34. [PMID: 28029445].
5. Betsholtz C. Insight into the physiological functions of PDGF through genetic studies in mice. Cytokine Growth Factor Rev 2004; 15:215-28. [PMID: 15207813].
6. Lindblom P, Gerhardt H, Liebner S, Abramsson A, Enge M, Hellstrom M, Backstrom G, Fredriksson S, Landegren U, Nystrom HC, Bergstrom G, Dejana E, Ostman A, Lindahl P, Betsholtz C. Endothelial PDGF-B retention is required for proper investment of pericytes in the microvessel wall. Genes Dev 2003; 17:1835-40. [PMID: 12897053].
7. Park DY, Lee J, Kim J, Kim K, Hong S, Han S, Kubota Y, Augustin HG, Ding L, Kim JW, Kim H, He Y, Adams RH, Koh GY. Plastic roles of pericytes in the blood-retinal barrier. Nat Commun 2017; 8:15296-[PMID: 28508859].
8. Takahashi K, Shimazawa M, Izawa H, Inoue Y, Kuse Y, Hara H. Platelet-Derived Growth Factor-BB Lessens Light-Induced Rod Photoreceptor Damage in Mice. Invest Ophthalmol Vis Sci 2017; 58:6299-307. [PMID: 29242904].
9. Siedlecki J, Asani B, Wertheimer C, Hillenmayer A, Ohlmann A, Priglinger C, Priglinger S, Wolf A, Eibl-Lindner K. Combined VEGF/PDGF inhibition using axitinib induces alphaSMA expression and a pro-fibrotic phenotype in human pericytes. Graefes Arch Clin Exp Ophthalmol 2018; 256:1141-9. [PMID: 29721663].
10. Mamer SB, Chen S, Weddell JC, Palasz A, Wittenkeller A, Kumar M, Imoukhuede PI. Discovery of High-Affinity PDGF-VEGFR Interactions: Redefining RTK Dynamics. Sci Rep 2017; 7:16439-[PMID: 29180757].
11. King R, Lu L, Williams RW, Geisert EE. Transcriptome networks in the mouse retina: An exon level BXD RI database. Mol Vis 2015; 21:1235-51. [PMID: 26604663].
12. Chesler EJ, Lu L, Wang J, Williams RW, Manly KF. WebQTL: rapid exploratory analysis of gene expression and genetic networks for brain and behavior. Nat Neurosci 2004; 7:485-6. [PMID: 15114364].
13. Beronja S, Livshits G, Williams S, Fuchs E. Rapid functional dissection of genetic networks via tissue-specific transduction and RNAi in mouse embryos. Nat Med 2010; 16:821-7. [PMID: 20526348].
14. Zhou DX, Zhao Y, Baker JA, Gu Q, Hamre KM, Yue J, Jones BC, Cook MN, Lu L. The effect of alcohol on the differential expression of cluster of differentiation 14 gene, associated pathways, and genetic network. PLoS One 2017; 12:e0178689-[PMID: 28575045].
15. Geisert EE, Lu L, Freeman-Anderson NE, Templeton JP, Nassr M, Wang X, Gu W, Jiao Y, Williams RW. Gene expression in the mouse eye: an online resource for genetics using 103 strains of mice. Mol Vis 2009; 15:1730-63. [PMID: 19727342].
16. Freeman NE, Templeton JP, Orr WE, Lu L, Williams RW, Geisert EE. Genetic networks in the mouse retina: growth associated protein 43 and phosphatase tensin homolog network. Mol Vis 2011; 17:1355-[PMID: 21655357].
17. Chesler EJ, Lu L, Shou S, Qu Y, Gu J, Wang J, Hsu HC, Mountz JD, Baldwin NE, Langston MA, Threadgill DW, Manly KF, Williams RW. Complex trait analysis of gene expression uncovers polygenic and pleiotropic networks that modulate nervous system function. Nat Genet 2005; 37:233-42. [PMID: 15711545].
18. Keane TM, Goodstadt L, Danecek P, White MA, Wong K, Yalcin B, Heger A, Agam A, Slater G, Goodson M, Furlotte NA, Eskin E, Nellaker C, Whitley H, Cleak J, Janowitz D, Hernandez-Pliego P, Edwards A, Belgard TG, Oliver PL, McIntyre RE, Bhomra A, Nicod J, Gan X, Yuan W, van der Weyden L, Steward CA, Bala S, Stalker J, Mott R, Durbin R, Jackson IJ, Czechanski A, Guerra-Assuncao JA, Donahue LR, Reinholdt LG, Payseur BA, Ponting CP, Birney E, Flint J, Adams DJ. Mouse genomic variation and its effect on phenotypes and gene regulation. Nature 2011; 477:289-94. [PMID: 21921910].
19. Homayouni R, Heinrich K, Wei L, Berry MW. Gene clustering by latent semantic indexing of MEDLINE abstracts. Bioinformatics 2005; 21:104-15. [PMID: 15308538].
20. Liao Y, Wang J, Jaehnig EJ, Shi Z, Zhang B. WebGestalt 2019: gene set analysis toolkit with revamped UIs and APIs. Nucleic Acids Res 2019; 47:W1W199-205. [PMID: 31114916].
21. Benjamni Y, Hochberg Y, Benjamini Y. Controlling the false discovery rate: a practical and powerful approach to multiple testing. J R Stat Soc B 1995; 57:289-300. .
22. Szklarczyk D, Gable AL, Lyon D, Junge A, Wyder S, Huerta-Cepas J, Simonovic M, Doncheva NT, Morris JH, Bork P, Jensen LJ, Mering CV. STRING v11: protein-protein association networks with increased coverage, supporting functional

discovery in genome-wide experimental datasets. Nucleic Acids Res 2019; 47:D1D607-13. [PMID: 30476243].

23. Zehetner C, Kirchmair R, Neururer SB, Kralinger MT, Bechrakis NE, Kieselbach GF. Systemic upregulation of PDGF-B in patients with neovascular AMD. Invest Ophthalmol Vis Sci 2014; 55:337-44. [PMID: 24334449].

24. Khawaja AP, Cooke Bailey JN, Wareham NJ, Scott RA, Simcoe M, Igo RP Jr, Song YE, Wojciechowski R, Cheng CY, Khaw PT, Pasquale LR, Haines JL, Foster PJ, Wiggs JL, Hammond CJ, Hysi PG, Eye UKB, Vision C, Consortium N. Genome-wide analyses identify 68 new loci associated with intraocular pressure and improve risk prediction for primary open-angle glaucoma. Nat Genet 2018; 50:778-82. [PMID: 29785010].

25. He JL. Platelet-derived growth factor-BB is involved in mesenchymal stem cell secretome-induced neuroprotection of retinal ganglion cells. Brain 2014; 137:e276-.

26. Steiger JL, Bandyopadhyay S, Farb DH, Russek SJ. cAMP response element-binding protein, activating transcription factor-4, and upstream stimulatory factor differentially control hippocampal GABABR1a and GABABR1b subunit gene expression through alternative promoters. J Neurosci 2004; 24:6115-26. [PMID: 15240803].

27. Wortel IMN, van der Meer LT, Kilberg MS, van Leeuwen FN. Surviving Stress: Modulation of ATF4-Mediated Stress Responses in Normal and Malignant Cells. Trends Endocrinol Metab 2017; 28:794-806. [PMID: 28797581].

28. Malabanan KP, Sheahan AV, Khachigian LM. Platelet-derived growth factor-BB mediates cell migration through induction of activating transcription factor 4 and tenascin-C. Am J Pathol 2012; 180:2590-7. [PMID: 22507839].

29. Shen J, Yang X, Xie B, Chen Y, Swaim M, Hackett SF, Campochiaro PA. MicroRNAs Regulate Ocular Neovascularization. Mol Ther 2008; 16:1208-16. [PMID: 18500251].

30. van Mil A, Grundmann S, Goumans MJ, Lei Z, Oerlemans MI, Jaksani S, Doevendans PA, Sluijter JP. MicroRNA-214 inhibits angiogenesis by targeting Quaking and reducing angiogenic growth factor release. Cardiovasc Res 2012; 93:655-65. [PMID: 22227154].

31. Bhootada Y, Kotla P, Zolotukhin S, Gorbatyuk O, Bebok Z, Athar M, Gorbatyuk M. Limited ATF4 Expression in Degenerating Retinas with Ongoing ER Stress Promotes Photoreceptor Survival in a Mouse Model of Autosomal Dominant Retinitis Pigmentosa. PLoS One 2016; 11:e0154779-[PMID: 27144303].

32. Geng W, Qin F, Ren J, Xiao S, Wang A. Mini-peptide RPL41 attenuated retinal neovascularization by inducing degradation of ATF4 in oxygen-induced retinopathy mice. Exp Cell Res 2018; 369:243-50. [PMID: 29803741].

33. Oskolkova OV, Afonyushkin T, Leitner A, von Schlieffen E, Gargalovic PS, Lusis AJ, Binder BR, Bochkov VN. ATF4-dependent transcription is a key mechanism in VEGF up-regulation by oxidized phospholipids: critical role of oxidized sn-2 residues in activation of unfolded protein response. Blood 2008; 112:330-9. [PMID: 18451308].

34. LeBlanc ME, Wang W, Chen X, Ji Y, Shakya A, Shen C, Zhang C, Gonzalez V, Brewer M, Ma JX, Wen R, Zhang F, Li W. The regulatory role of hepatoma-derived growth factor as an angiogenic factor in the eye. Mol Vis 2016; 22:374-86. [PMID: 27122967].

35. Hollander A, D'Onofrio PM, Magharious MM, Lysko MD, Koeberle PD. Quantitative retinal protein analysis after optic nerve transection reveals a neuroprotective role for hepatoma-derived growth factor on injured retinal ganglion cells. Invest Ophthalmol Vis Sci 2012; 53:3973-89. [PMID: 22531700].

36. Rieg AD, Suleiman S, Anker C, Verjans E, Rossaint R, Uhlig S, Martin C. PDGF-BB regulates the pulmonary vascular tone: impact of prostaglandins, calcium, MAPK- and PI3K/AKT/mTOR signalling and actin polymerisation in pulmonary veins of guinea pigs. Respir Res 2018; 19:120-[PMID: 29921306].

37. Mamer SB, Chen S, Weddell JC, Palasz A, Wittenkeller A, Kumar M, Imoukhuede PI. Discovery of High-Affinity PDGF-VEGFR Interactions: Redefining RTK Dynamics. Sci Rep 2017; 7:16439-[PMID: 29180757].

Articles are provided courtesy of Emory University and the Zhongshan Ophthalmic Center, Sun Yat-sen University, P.R. China. The print version of this article was created on 19 June 2020. This reflects all typographical corrections and errata to the article through that date. Details of any changes may be found in the online version of the article.